Paramagnetic Resonance Absorption in Salts of V and Mn†

CLYDE A. HUTCHISON, JR., AND LEONARD S. SINGER*
Institute for Nuclear Studies and Department of Chemistry, University of Chicago, Chicago, Illinois
(Received July 29, 1952)

Paramagnetic resonance absorptions in tetravalent, trivalent, and divalent salts of V and in a divalent salt of Mn have been investigated at room temperature and at a frequency of 9.2×10^9 sec^{-1}. A detailed study has been made of the absorption in single crystals of the Tutton salt of V^{+2} as a function of orientation. The results have been interpreted on the basis of crystalline electrostatic fields.

INTRODUCTION

WE have carried out an investigation of paramagnetic resonance absorption at a frequency of 9.2×10^9 sec^{-1} and at room temperatures in tetravalent, trivalent, and divalent salts of V and in a divalent salt of Mn. We have studied in particular detail the case of the Tutton salt of divalent V. During the preparation of our results for publication there appeared the work of Bleaney, Ingram, and Scovil[1] on this same salt at a frequency of 2.3×10^{10} sec^{-1}. We consequently present here an abbreviated account of our work.[2]

EXPERIMENTAL WORK

Preparation of Powders

The tetravalent salt of V studied was a commercial product labeled cp, G. Frederick Smith and Company $VOSO_4\cdot2H_2O$, which was dried at 110°C for 24 hr. Analysis showed that this salt contained no other transition elements and no other valence states of V, but did contain small amounts of $(NH_4)_2SO_4$ and H_2SO_4.

TABLE I. Description of cylindrical crystals.

Crystal No.	Weight g	Density g cm^{-3}	% V	% of metal atoms which are V	Angle between cylindrical axis and a-axis	b-axis (Symmetry axis)	c-axis
1							
Outer section	0.2554	···	4.64	36.1	···	···	···
Middle section	0.3307	···	4.54	35.3	···	···	···
Inner section	0.1709	···	4.81	37.4	···	···	···
Whole crystal	0.8217	1.898	4.66	36.3	0.500π	0.000	0.500π
2	0.6009	1.894	4.66	36.3	0.068π	0.500π	0.524π
3	0.5559	1.894	4.66	36.3	0.068π	0.500π	0.524π
4	0.8080	1.895	4.52	35.2	0.568π	0.500π	0.024π

Two trivalent salts of V were prepared[3] by reduction of a solution of cp V_2O_5 in H_2SO_4 to the tetravalent state with SO_2 followed by electrolytic reduction to the trivalent form and precipitation with concentrated H_2SO_4. This produced a salt which analysis showed to have composition very close to $V_2(SO_4)_3\cdot2H_2SO_4\cdot6H_2O$ and to contain no other valence states of V. Heating of this salt under reduced pressure produced a second material containing 19.7 percent V instead of 14.8 percent which the initial preparation contained.

The divalent Tutton salt, $V(NH_4)_2(SO_4)_2\cdot6H_2O$ was prepared in solution by a method similar to that of Meyer and Aulich.[4] The solution was evaporated on a vacuum line to give a solid product which analysis showed to have the composition V, 13.1 percent; SO_4, 51.2 percent; mole SO_4/mole V, 2.07. The theoretical composition is V, 13.2 percent; SO_4, 49.2 percent; mole SO_4/mole V, 2.00. Successive oxidations with $KMnO_4$ and reduction with SO_2 showed that of the total V, a maximum of 11 percent V^{+3} or 6 percent V^{+4} or 4 percent V^{+5} or some equivalent combination of the three was present.

Preparation of Crystals

Single crystals of $V(NH_4)_2(SO_4)_2\cdot6H_2O$ were prepared from aqueous solution by the method of Holden.[5] Since V^{+2} reduces H_2O, it was necessary to add amalgamated Zn to the solutions from which the crystals were grown in order to keep the V in the divalent state for the several weeks required for growth. This introduced Zn^{+2} into the crystals. The monoclinic Tutton salts of V^{+2} and Zn^{+2} are isomorphous. The descriptions of four such mixed crystals of the Tutton salts of Zn and V, after grinding to right circular cylinders are given in Table I.

Goniometric measurements on the mixed monoclinic crystals gave a value of 106° 16′ for the β-angle between the a and c axes and 0.737:1.000:0.496 for the axial ratios, $a:b:c$. These are very close to the values found for the Tutton salts of Ni, Mg, Zn, and Fe.[6] The a, b,

† Assisted by the ONR.
* Now at the Naval Research Laboratory, Washington, D. C.
[1] Bleaney, Ingram, and Scovil, Proc. Phys. Soc. (London) A64, 601 (1951).
[2] For detailed paper (or extended version or material supplementary to this article) order Document 3731 from American Documentation Institute, 1719 N Street, N.W., Washington 6, D. C., remitting $2.30 for microfilm (images 1 inch high on standard 35-mm motion picture film) or $22.80 for photocopies (6x8 inches) readable without optical aid.
[3] A. Stahler and H. Wirthwein, Ber. deut. chem. Ges. 38, 3978 (1905).
[4] J. Meyer and M. Aulich, Z. anorg. u. allgem. Chem. 194, 278 (1930).
[5] A. N. Holden, Disc. Faraday Soc. No. 5, 312 (1949).
[6] *Strukturbericht*, edited by C. Hermann *et al.* (Becker and Eiler, Leipzig), Vol. 2 (1928–32), p. 436.

and c axes will throughout this paper be taken as forming a right-hand set.

After goniometric alignment a surface grinder was employed to produce a plane surface on the crystal normal to the desired direction of the cylindrical axis. This plane surface was then cemented to a holder and a right circular cylindrical surface was ground. At least one crystal edge was left on the end opposite the plane. This was employed to mount the cylindrical crystal on a crystal holder at a known angle of rotation about the axis with respect to the graduated head of the holder. The dial reading of the crystal holder could thus be correlated with the angles between axes of the crystal and the direction of the alternating and the static magnetic fields. The maximum error in the determination of angles throughout this work is approximately 0.010π.

Crystals of $Mn(NH_4)_2(SO_4)_2\cdot 6H_2O$ were prepared and mounted in the same manner as described for the case of the V salt. Crystal 1 was the pure Mn salt with the cylindrical axis parallel to the b axis.

Apparatus

The right circular cylindrical crystals were mounted in a transmission cavity in the form of a rectangular box operated in the TE_{102} mode at a frequency of approximately 9×10^9 sec^{-1}. The cylindrical axis was maintained parallel to the broad face of the guide and perpendicular to the narrow face and the longitudinal axis of the guide. The holder was graduated and rotatable so that the crystal could be rotated through known angles about its axis.

The klystron was modulated at an audiofrequency with a square wave and the detected transmitted microwave power was amplified with a tuned amplifier. The detected output of the amplifier was either read from a meter or recorded with a recording potentiometer. The magnetic field was measured as a function of current using the proton resonance. Magnetic fields as determined by measurement of the current were reproducible to 0.1 percent.

RESULTS

Tetravalent V

This powder showed a single strong resonance absorption with a maximum corresponding to a g factor of 1.96 and a width at half-maximum absorption of 180 gauss.

Trivalent V

No magnetic resonance absorption was observable in either of the two preparations.

Divalent V

The powder gave the rather complicated absorption shown in Fig. 1.

Crystal 1 was oriented such that the a axis, c axis, direction of propagation of microwaves and direction of static field were coplanar. In Fig. 2 are shown the absorptions for various values of ψ. ψ is the angle of rotation of the c axis away from the direction of propagation of microwaves in the sense in which a right hand screw would be turned to advance it along the b axis of the crystal. Plotted on the vertical axis is the quantity $(B-A)/(B-Z)$, in which A is amplifier output at field strength H; B is amplifier output at very high field strength; Z is amplifier output with infinite attentuation in microwave transmission line. A second crystal cut in the same manner and not described in Table I gave results in agreement with those of Fig. 2.

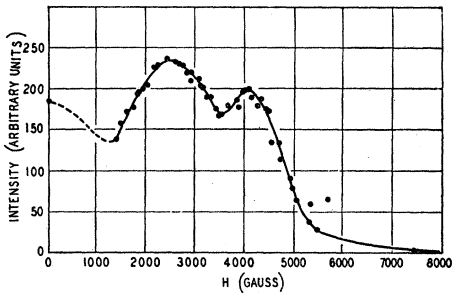

FIG. 1. Experimental intensity of absorption as a function of magnetic field strength.

Crystal 3, cut as stated in Table I, was examined at 26 different values of the angle η between the b axis and the direction of the static magnetic field. The absorptions were recorded by a recording potentiometer. Measurements on crystal 2 were in agreement with those on crystal 3.

Absorptions due to crystal 4 at 23 different values of the angle σ, between the b axis and the direction of propagation of microwaves in the wave guide were recorded.

A crystal in which only 7.4 percent of the metal ions were V gave, when rotated about its b axis, essentially the same absorption curves as crystal 1.

Mn

Crystal 1 gave the absorptions shown in Fig. 3.

INTERPRETATION OF RESULTS

Powders

The observations on the paramagnetic resonance absorption of the various oxidation states of V are consistent with the rule of Kramers.[7]

Crystals

a. Calculations

We have employed for the interpretation of the data the model employed by Hebb and Purcell;[8] Weiss, Whitmer, Torrey, and Hsiang;[9] Whitmer, Weidner,

[7] H. A. Kramers, Proc. Roy. Acad. Amsterdam 4, 871 (1937).
[8] M. H. Hebb and E. M. Purcell, J. Chem. Phys. 5, 338 (1937).
[9] Weiss, Whitmer, Torrey, and Hsiang, Phys. Rev. 72, 975 (1947).

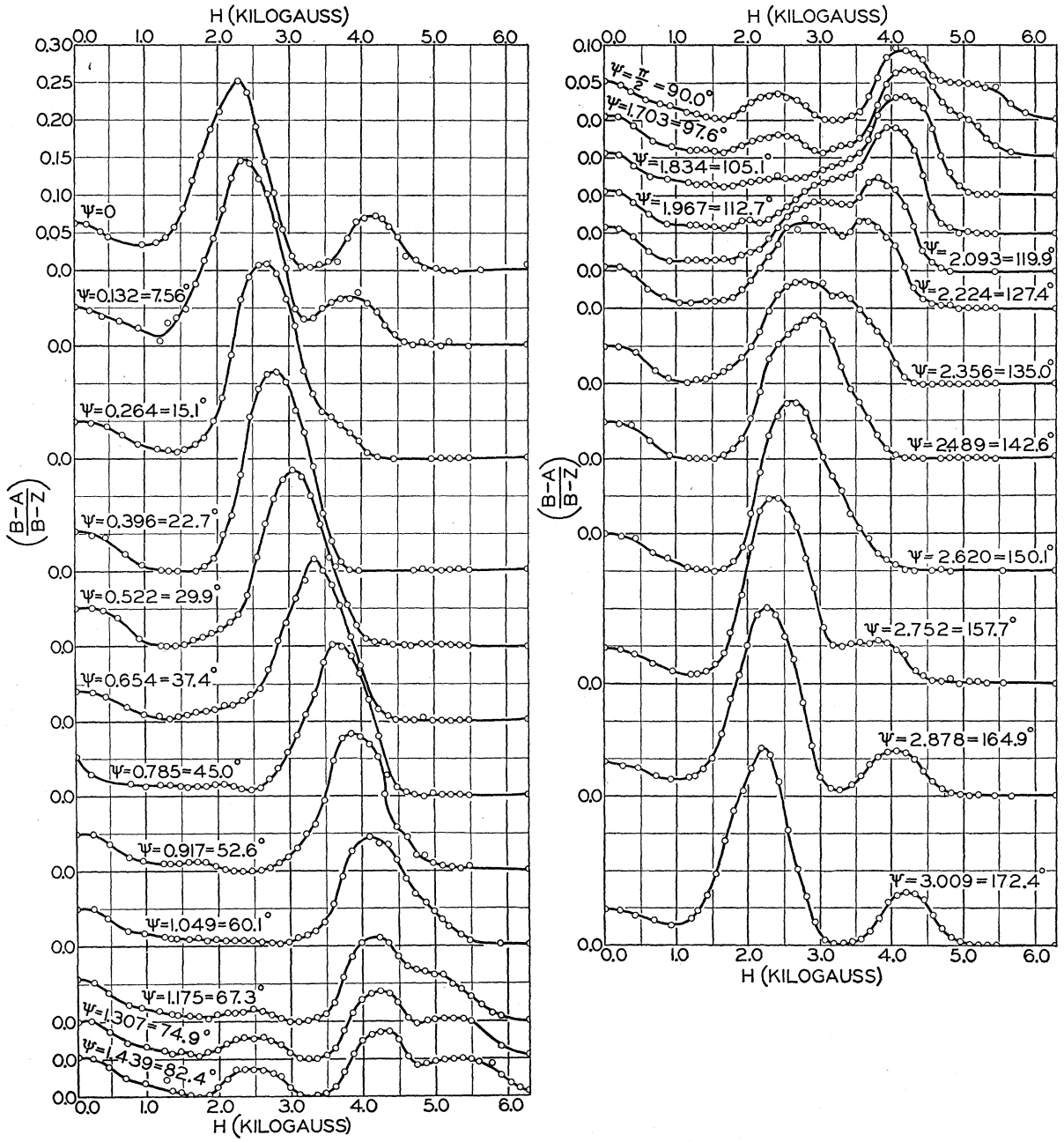

FIG. 2. Experimental intensity of absorption as a function of magnetic field strength.

and Weiss;[10] Bleaney, Penrose, and Plumpton[11] and others in the interpretation of the magnetic properties of alums and Tutton salts. The Hund ground state of V^{+2} is ^4F. The crystalline structure is assumed similar to that known for the Mg salt,[12] and the space group is assumed to be $C_{2h}{}^5$. The large electric field of the nearly octahedral arrangement of H_2O dipoles results in a Γ_2 ground state with only spin degeneracy.[13] A small axial electric component, due to distortion of the octahedron, combined with spin-orbit coupling is assumed to result in a further splitting of the Γ_2 state by an amount δ with only the Kramers degeneracy remaining to be removed by the static magnetic field. There are two inequivalent V^{+2} ions per unit cell. The axial electric fields for these two ions differ only with respect to the angle which they make with the b axis of the monoclinic

[10] Whitmer, Weidner, and Weiss, Phys. Rev. **73**, 1468 (1948).
[11] Bleaney, Penrose, and Plumpton, Proc. Roy. Soc. (London) **A198**, 406 (1949).
[12] W. Hoffman, Z. Krist. **78**, 279 (1931).
[13] H. A. Bethe, Ann. Physik **3**, 133 (1929).

crystal, the one being a reflection of the other in a plane perpendicular to the b axis. The secular equation[9,10,14] of the combined axial electric-spin-orbit and magnetic perturbations is

$$\epsilon^4-\tfrac{1}{2}\epsilon^2(1+20x^2)+4\epsilon x^2(1-3\cos^2\theta)+1/16+9x^4+\tfrac{1}{2}x^2-3x^2\cos^2\theta=0.$$

In this equation $x=g\beta H/2\delta$, $\epsilon=E/\delta$, θ is the angle between the magnetic field and the electric axis, and E is the eigenvalue of the energy. For three values of θ, 0, $\cos^{-1}(1/\sqrt{3})$, and $\pi/2$, this equation factors into two quadratics. For other values of θ, since the equation is quadratic in x^2, we may easily calculate the eigenvalues of the energy *versus* static field strength in terms of the one parameter δ. We calculated such energy level curves (ϵ *versus* x) for θ ranging from 0 to $\pi/2$ at intervals of about every $\pi/24$. We have also graphed the $\Delta\epsilon$'s *versus* x and the values of H for maximum absorption (resonance) *versus* δ for the same values of θ as an aid in the interpretation of the results. Moreover, we have also calculated the perturbed eigenstates and the matrix elements of J_z and of $J_+=J_x+iJ_y$ as functions of x, where the z axis is the axis of the axial electric perturbation.[14] From these we have calculated for several values of the angle θ, the value of

$$|(M'|J_{z'}|M)|^2=(M'|J_z|M)\cos^2\xi+\tfrac{1}{4}\cos^2\xi\cot^2\theta[(M'|J_+|M)+(M'|J_+|M')]^2+\tfrac{1}{4}\cos^2\beta\csc^2\theta[(M'|J_+|M)-(M|J_+|M')]^2-(\cos^2\xi)(\cot\theta)(M'|J_z|M)[(M'|J_+|M)+(M|J_+|M')]$$

as a function of x. This is the square of the matrix element of the component of the angular momentum along the z' axis in a new system of coordinates oriented as follows with respect to the set x, y, z (in which J was expressed): z' is the direction of the high frequency magnetic field, y' is the direction of the static magnetic field and x' is the direction of propagation of microwave energy along the wave guide. The x and y axes being arbitrary are so chosen that the projection of y' on the x, y plane lies along x. ξ is the angle between z and z', β the angle between z and x' and θ the angle between z and y' (this is the same θ as previously defined). Hence $|(M'|J_{z'}|M)|^2$ is proportional to the intensity of the absorption due to the transition $M'\rightarrow M$. Graphs of $|(M'|J_{z'}|M)|^2$ *versus* x were employed in the comparison of the experimental relative intensities with the model.

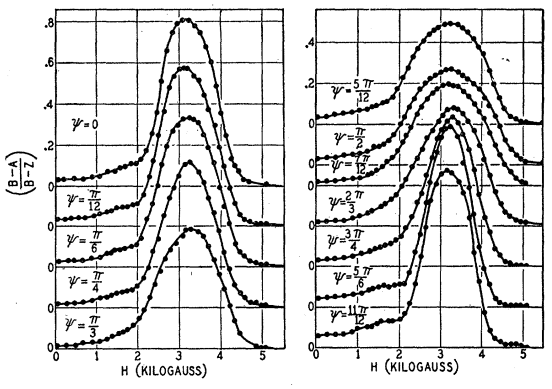

FIG. 3. Experimental intensity of absorption as a function of magnetic field strength.

[14] C. Kittel and J. M. Luttinger, Phys. Rev. **73**, 162 (1948).

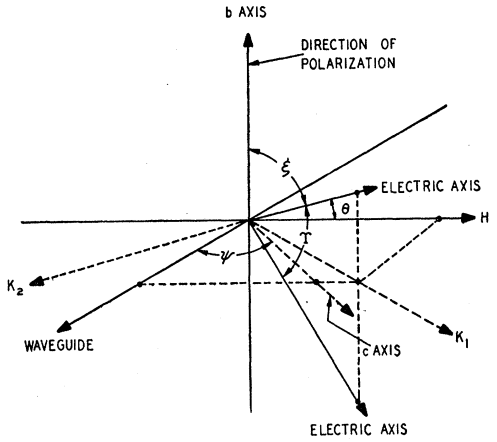

FIG. 4. Orientation of crystal.

b. *The Orientation of the Electric Axes*

It is clear that in the measurements on V^{+2} crystal 1 (see Table I, Fig. 2), oriented as shown in Fig. 4 the electric axes of the two inequivalent V^{+2} ions have the same value of $\cos^2\theta$. Hence since θ enters into the secular equation only as $\cos^2\theta$ the resonance pattern is thereby simplified. In Fig. 5(a) are shown the peak positions as a function of ψ as determined from Fig. 2. Examination of this plot showed that there were two stationary points $\pi/2$ apart, one at $\psi=0.476\pi$ and one at $\psi=0.976\pi$. It was therefore concluded that at one of these angles the plane of the electric axes was perpendicular to and at the other parallel to the magnetic field corresponding to the two points of symmetry in the function $\cos^2\theta$ occurring in the secular equation. Consequently the orientations of the principal axes, K_1, K_2, of susceptibility shown in Fig. 4 (K_1 is in the plane of the electric axes and bisects the angle between them and K_2 is perpendicular to their plane) are known except for a rotation of $\pi/2$ in the a, c plane. It was assumed (this assumption will later be seen to be correct) that when $\psi=0.976\pi$ the plane of the electric axes, and hence K_1, was perpendicular to the magnetic field.

In order to test this assumption crystals 2 and 3 (see Table I) were cut so that their cylindrical axes were perpendicular to this assumed plane of the electric axes. The required angles were those listed in Table I. The crystal was oriented in the wave guide as shown in Fig. 6. In Fig. 7(a) are shown the experimental peak positions as determined from the recorded absorption

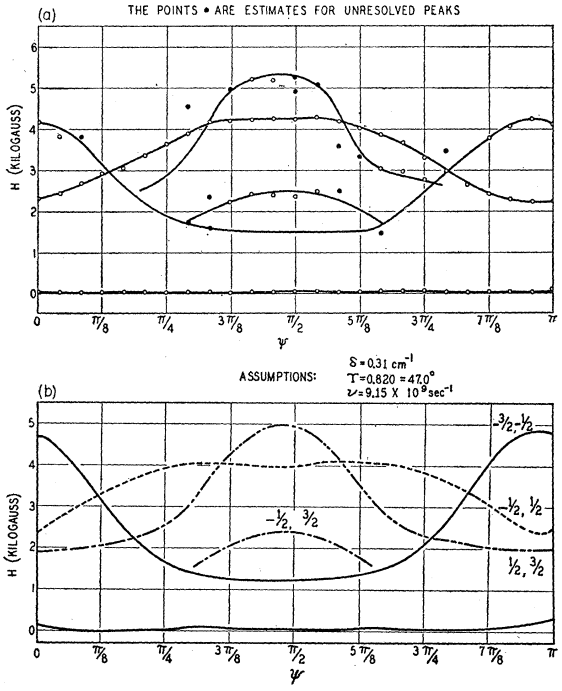

FIG. 5. Field strength for maximum absorption as a function of ψ. (a) Experimental; (b) Theoretical.

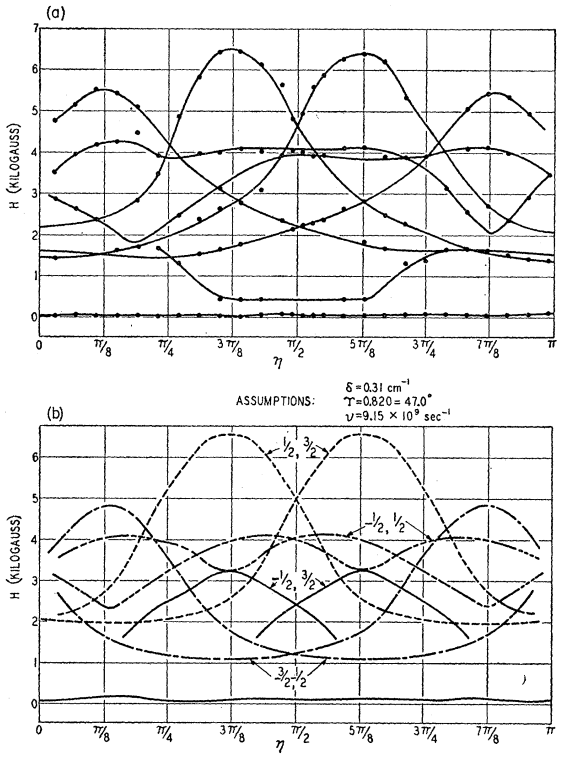

FIG. 7. Field strength for maximum absorption as a function of η. (a) Experimental; (b) Theoretical.

curves. Examination of this plot showed that there were four stationary points, two of them 0.261π apart and located symmetrically about $\eta=0.500\pi$, and the other two $\pi(1-0.261)$ apart located symmetrically about $\eta=0.500\pi$. This then is seen to determine the acute angle Υ, between the electric axes as 0.261π and they consequently make angles of 0.369π and -0.369π with the b axis.

As a check on this hypothesis crystal 4 (see Table I) was cut so that its cylindrical axis was the K_1 axis (the bisector of the acute angle made by the electric axes). The required angles were those listed in Table I. The crystal was oriented as shown in Fig. 8. In Fig. 9(a) are shown the experimental peak positions as determined from the recorded absorption curves. Examination of this plot showed that the cylindrical axis of this crystal was in fact K_1. Since there are only two stationary points, it is indicated that the electric axes associated with the inequivalent ions made angles θ and $-\theta$ with the static magnetic field, and that both kinds of ions gave rise to the same absorption spectrum, as was to be expected.

c. *The Magnitude of the Electric Field Splitting* δ

Knowing that the angle Υ between the electric axes was 0.261π, it was then desired to adjust the parameter

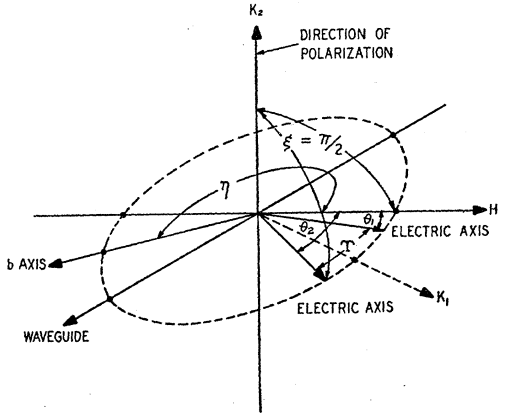

FIG. 6. Orientation of crystal.

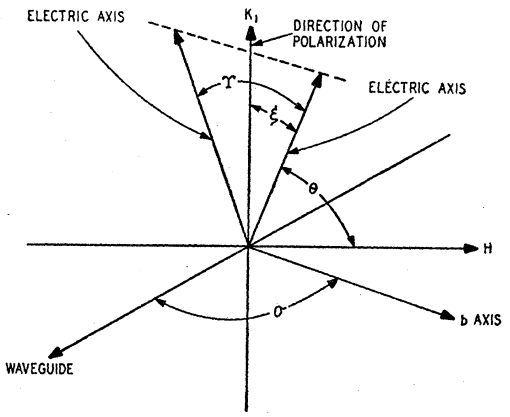

FIG. 8. Orientation of crystal.

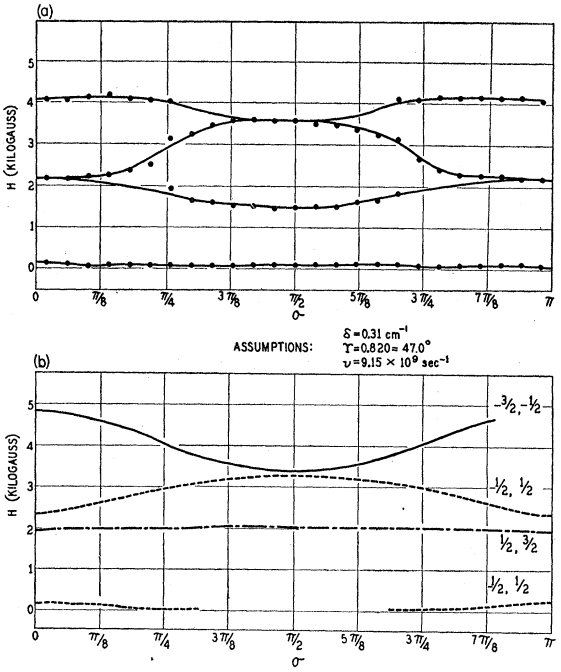

FIG. 9. Field strength for maximum absorption as a function of σ. (a) Experimental; (b) Theoretical.

δ so that the best fit of the experiments with the theory could be obtained. As a first step the calculated graphs of peak positions and intensities *versus* field strength as described in Sec. *a* were employed to construct theoretical resonance absorption curves for several values of θ. In constructing these curves the shapes were assumed Gaussian and the experimental widths were employed as these were substantially larger than the theoretical ones. The theoretical and experimental curves for $\delta=0.31\ \text{cm}^{-1}$ are compared for $\theta=0.131\pi$, $\theta=\cos^{-1}(1/\sqrt{3})$, and $\theta=\pi/2$ in Figs. 10, 11, and 12, respectively. The strong field quantum numbers are employed for the labeling of these figures. The experimental curves were taken from those on crystal 1 shown in Fig. 2 since in this orientation (see Fig. 4) both axes have the same

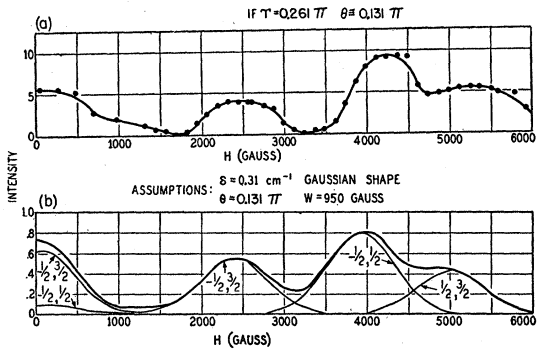

FIG. 10. Intensity of absorption as a function of field strength for $\psi=\pi/2$. (a) Experimental; (b) Theoretical.

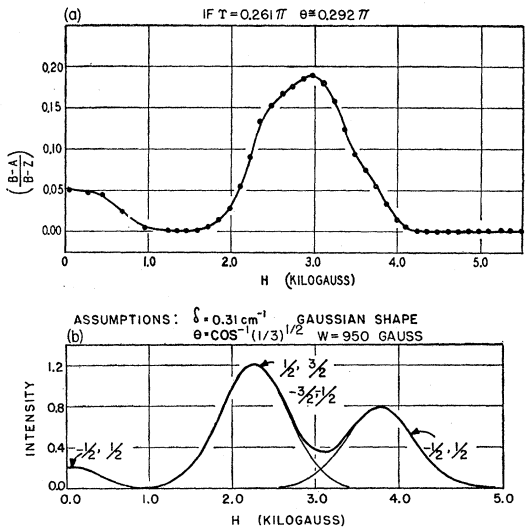

FIG. 11. Intensity of absorption as a function of field strength for $\psi=0.794\pi$. (a) Experimental; (b) Theoretical.

value of $\cos^2\theta$ and hence both inequivalent ions give rise to the same absorption pattern. It was found that any value of δ less than the microwave quantum, 0.306 cm^{-1}, yielded curves with very intense absorptions near zero magnetic field, in disagreement with the experimental observations. For values of δ above 0.306 cm^{-1} the disagreement between theory and experiment increased with increasing δ. In view of an insensitivity in the choice of δ of about 0.01 cm^{-1} the value $\delta=0.31\pm0.01\ \text{cm}^{-1}$ was chosen.

As a second step this value of δ was employed in

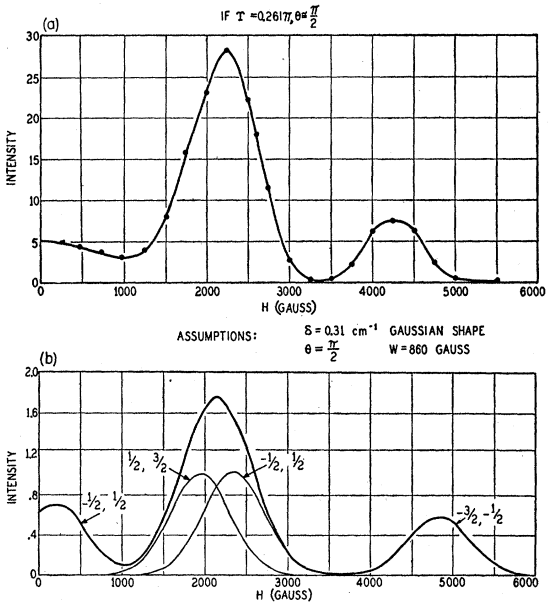

FIG. 12. Intensity of absorption as a function of field strength for $\psi=0$. (a) Experimental; (b) Theoretical.

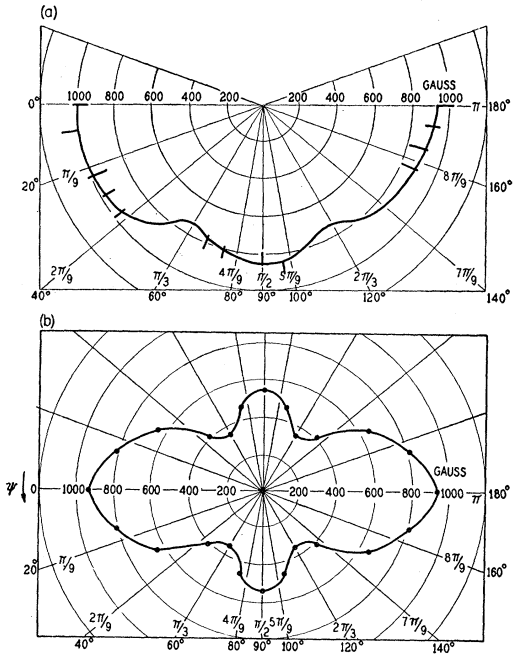

FIG. 13. Width at half-maximum absorption as a function of ψ. (a) Experimental; (b) Theoretical.

conjunction with the previously determined values, 0.261π for Υ, and 0.024π for the dihedral angle between the plane of the electric axes and the b, c plane (i.e., between K_1 and c axis) to construct theoretical curves of field strengths for maximum absorption *versus* angle of rotation. These curves are shown in Figs. 5(b), 7(b), and 9(b) for the angles $\theta=0.131\pi$, $\theta=\cos^{-1}(1/\sqrt{3})$, and $\theta=\pi/2$, respectively. The strong field quantum numbers are employed for the labeling of these figures. The corresponding Figs. 5(a), 7(a), and 9(a) are the experimental curves for the same angles obtained from crystal 1 for which both inequivalent ions gave rise to the same absorption curve.

Positions of peaks and relative intensities are seen to be in essential agreement with the theoretical results. The rather large discrepancy in the appearance of the experimental and theoretical absorption curves at $\theta=\cos^{-1}(1/\sqrt{3})$ is seen on examination of Fig. 2 to occur in a region where the appearance is changing extremely rapidly with rotation of the crystal and hence is very sensitive to choice of angles. The theoretical curve is not constructed for exactly the experimental angle.

d. Width

In Fig. 13 the experimental widths at half-maximum absorption are plotted *versus* the angle of rotation ψ for the experiments using crystal 1. The theoretical curve calculated from the theory of Van Vleck[15] assuming Gaussian shape and the data of Hoffman for the pure V salt are also shown in Fig. 13. For the concentrations of V employed, the theoretical widths are considerably less than this being 330 gauss when the c axis is parallel to the magnetic field. Thus, the dipole-dipole interactions alone are not sufficient to account for the observed widths. Also, as has been stated previously, a considerably more dilute crystal (by a factor of about 5) showed essentially the same widths as those for the more concentrated crystals. These abnormal widths are presumably due to nuclear interactions leading to unresolved hyperfine structure.

CONCLUSIONS

The results of the measurements of the resonance absorptions in the V Tutton salt are in essential agreement with a model based on the known structure of the Tutton salts. Small axial electric fields superposed on the large cubic fields about the two inequivalent V^{+2} ions lead to this agreement when the axial splitting parameter δ is taken to be 0.31 ± 0.01 cm^{-1}; the smaller angle Υ between the electric axes is taken to be 0.261π; and the dihedral angle between the plane of the electric axes and the b, c plane (i.e., the angle between K_1 and the c axis) is taken to be 0.024π. K_1 lies within the angle β between the a and c axes. The small discrepancies which exist between this simple model and the observations are undoubtedly due to the actual rhombicity of the electric field as discussed by Bleaney, Ingram, and Scovil.[1] These authors employed a much more dilute salt, one V ion per 1000 metal ions, than was used in our experiments (see Table I). They made their measurements at 1.2 cm wavelength and 20° or 90°K whereas our observations were at 3 cm and room temperature. However, they obtained 0.244π for the angle between electric axes to be compared with our value, 0.261π; and 0.01π for the angle between K_1 and the c axis to be compared with our value, 0.024π. Their axial splitting parameter $2D=0.316\pm0.01$ cm^{-1} is to be compared with our value, 0.31 ± 0.01 cm^{-1}.

We thank Philip Shevick for the design and construction of electronic equipment and Hans Riehm and Jay S. Hitchcock for the construction of apparatus.

[15] J. H. Van Vleck, Phys. Rev. **74**, 1168 (1948).